Joint EPRI – 123HiMAT International Conference on
Advances in High Temperature Materials
October 21–24, 2019, Nagasaki, Japan
J. Shingledecker, M. Takeyama, editors
https://doi.org/10.31339/asm.cp.am-epri-2019p0506

INFLUENCE OF γ' MORPHOLOGY ON HOT WORKABILITY OF ALLOY U520 BELOW THE γ'-SOLVUS TEMPERATURE

Yoshiki KUMAGAI, Yoshinori SUMI, Hiroyuki TAKABAYASHI
Research & Development Center, Daido Steel Co., Ltd.
2-30 Daido-cho, Minami-ku, Nagoya 457-8545, Japan

ABSTRACT

The relationship between the hot workability and the precipitation morphology of γ′ phase in the Alloy U520 was examined with a focus on the presence of γ′-nodule. To change the morphology of γ' phase, forged bars of the Alloy U520 were solution treated followed by cooling process with the cooling rates of 5~100 K/h. After the heat treatment, both γ' phases of intragranular particle and nodule along grain boundaries were observed, and the both sizes increased by slowing down the cooling rate. That is, the area fraction of γ'-nodule increased from about 0.1 % in the sample cooled at 100 K/h to about 70 % at 5 K/h. In Gleeble tension test, the slow-cooled samples basically exhibited higher ductility than water-quenched samples below the γ′-solvus temperature. However, the ductility was maximized in the sample cooled at 20 K/h, and excessive decrease of cooling rate resulted in a drop in ductility. EBSD analysis revealed that dynamic recrystallization (DRX) was often occurred in grain interior but suppressed at γ′-nodule area, indicating that presence of γ′-nodule had a negative influence on hot workability at subsolvus temperature.

Keywords: Ni-based superalloy, hot ductility, cooling rate, precipitation morphology

INTRODUCTION

Hot workability of wrought Ni-based superalloys which contains high volume fraction of γ′ phase deteriorates drastically below the γ′-solvus temperature due to rapidly precipitation of fine γ′ particles. As one of methods to improve the workability, it was proposed that coarsening of the γ′ particles by slow cooling from above the γ′-solvus temperature before hot deformation process [1]. However, it is known that in some alloys with intermediate volume fraction of the γ′ phase such as Alloy U520, a γ′-nodule like precipitation (so-called "fan-type" γ-γ' structure in literatures) occurs from grain boundaries in the case of slower cooling rate [2-4]. It is reported that the presence of γ′-nodule would improve the hot ductility owing to grain boundary serration [5], however it is not clear that the relationship between volume fraction of the γ′-nodule and hot ductility. Therefore, in this study, influence of γ′ morphology on hot workability of the alloy U520 was examined with a focus on the presence of γ′-nodule.

EXPERIMENT

The chemical composition of the investigated Alloy U520 is shown in Table 1. The γ′-solvus temperature measured by DTA analysis for this material is approximately 1333 K. The forged

bars of the alloy were solution treated at 1378 K for 4 h followed by water-quenching or cooling directly from 1378 K with cooling rates of 5, 10, 20, 50, and 100 K/h (Fig. 1 (a)). The cooling process was interrupted at 1173 K to prevent precipitation of σ phase [6]. After the cooling, the bars were gas-quenched. The heat-treated samples were subsequently subjected to Gleeble test (a high speed tensile test). Test specimens with a gauge length of 20 mm and a diameter of 4.5 mm were prepared. The gauge portion of the specimens were heated to 1123 ~ 1473 K in 100 s and held for 60 s in a Gleeble tester, then pulled at 50.8 mm/s (strain rate is approximately 2.54 s^{-1}) (Fig. 1 (b)). Reduction of area was employed as a measure of hot ductility. The microstructures were examined by optical microscopy (OM), field emission-scanning electron microscopy (FE-SEM) and electron backscattered diffraction (EBSD) analysis. γ′ particle size and area fraction of γ′-nodule were analyzed by Image J software [7], using optical micrographs and backscattered electron images (BEIs).

Table 1: Chemical composition of Alloy U520 studied (in weight percent).

C	Cr	Mo	W	Co	Al	Ti	Ni
0.04	18.70	5.88	1.04	12.31	2.00	3.15	Bal.

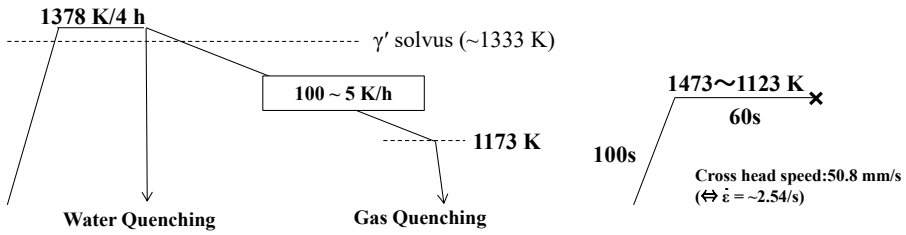

Figure 1: (a) Heat treatment condition and (b) Gleeble test condition.

RESULTS

Initial microstructure

Typical microstructures after heat treatment are shown in Fig. 2. Little amount of primary carbide or nitride are observed in water-quenched sample and the average grain size is about 110 μm (Fig. 2 (a)). In slow-cooled samples, γ′ precipitates are observed in grain interior and heterogeneous formation of γ′-nodules are observed in the vicinity of grain boundaries (Fig. 2 (b-c)). These γ′-nodules are formed in a manner of discontinuous precipitation, resulting in serration of grain boundaries. Table 2 shows average area fraction of γ′-nodule in slow-cooled samples. The area fraction of γ′-nodule slightly increases with slowing cooling rate down to 50 K/h. However, slower cooling rate results in remarkable increase of the area fraction and the 5 K/h-cooled sample shows approximately 70% volume fraction of γ′-nodule.

Figure 3 shows magnified microstructures of the slow-cooled samples. In grain interior, both the average size of γ′ particles (dark contrast) and its interparticle spacing increases with decreasing cooling rate. The γ′ particles show basically cuboidal shape, and slower cooling rate makes the morphology more irregular. On the other hand, γ′ precipitates in γ′-nodules show fiber-like or dendritic morphology and growth radially. The interparticle spacing between each γ′ fiber is smaller than the interparticle spacing in grain interior regardless of the cooling rate. Note that no carbide precipitation on grain boundaries during cooling process is observed in all specimens.

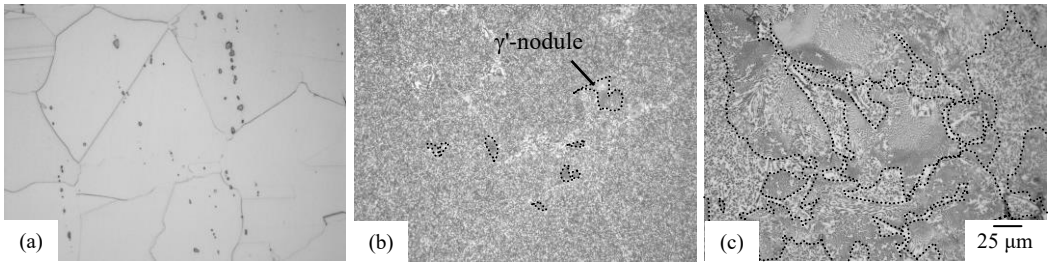

Figure 2: Optical micrographs of samples after solution treatment followed by (a) water quenching, (b) cooling at 50 K/h and (c) cooling at 10 K/h.

Table 2:Average area fraction of γ′-nodule for slow-cooled samples.

Cooling rate	(W.Q.)	100 K/h	50 K/h	20 K/h	10 K/h	5 K/h
Area fraction of γ′-nodule	-	0.001	0.02	0.21	0.60	0.73

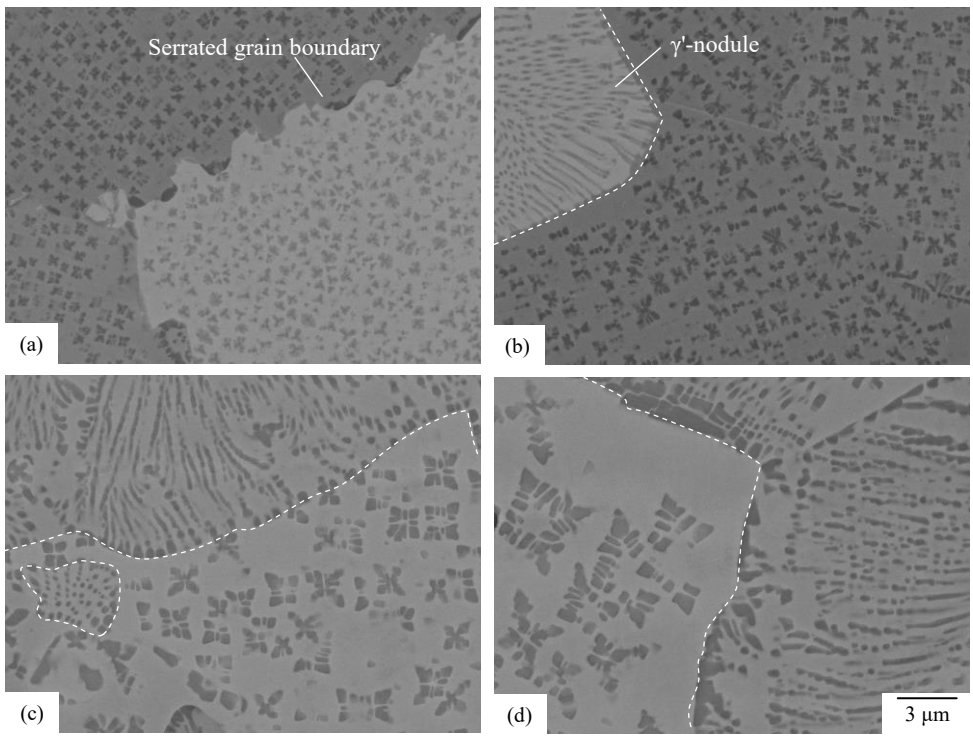

Figure 3: BEIs showing microstructures of samples after solution treatment followed by cooling at (a) 100 K/h, (b) 50 K/h, (c) 10 K/h and (d) 5 K/h.

Gleeble test

Figure 4 (a) shows reduction of area for water-quenched and slow-cooled specimens in Gleeble test. Ductility of the water-quenched specimens decreases drastically in the case of test temperatures fall below the γ′-solvus temperature (approximately 45 % at 1173 K). The slow-cooled specimens, on the other hand, show a gradual decrease of ductility below the γ′-solvus

temperature and keep the reduction of area over 60 % at 1173 K. It is clear that slow-cooling process before hot deformation is basically effective to improve hot workability at subsolvus temperature.

Figure 4 (b) shows reduction of area as a function of cooling rate in the initial cooling process. Hot ductility above 1273 K increases with decreasing cooling rate down to 20 K/h. However, lower cooling rate results in a drop in ductility and the reduction of area for the 5 K/h-cooled specimen is equal to the one for the 50 K/h-cooled specimen at 1173 K. Thus, there is an optimal cooling rate to maximize hot ductility at subsolvus temperature.

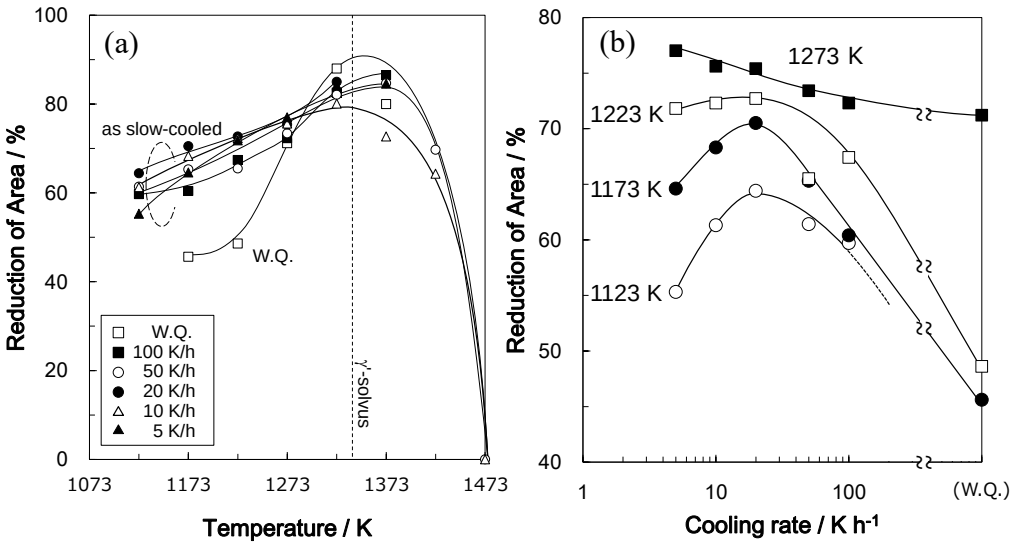

Figure 4: Reduction of area in Gleeble tension test as a function of (a) test temperature and (b) cooling rate in the initial heat treatment process.

DISCUSSION

To understanding the influence of γ′ precipitation morphology on hot ductility, deformed microstructures of the Gleeble test specimens tested at 1173 K were analyzed. At 1173 K, it is assumed that no additional precipitation of γ′ particles occurs expect for water-quenched specimen. Note that all tested specimens showed ductile fracture surface at 1173 K. Fig. 5 shows the cross-sectional microstructure of the Gleeble tested specimens and corresponding Inverse Pole Figure (IPF) maps for water-quenched and 10 K/h-cooled specimens. For the water-quenched specimen, deformed grains along tensile direction and strain contrasts are observed and no recrystallization has occurred (Fig. 5 (a-b)). This strain accumulation in grain interior would be caused by precipitation of fine γ′ particles during heating process before deformation. On the other hand, for 10 K/h-cooled specimen, recrystallized grains with a grain size of about 2 μm are observed around deformed coarse γ′ particles in grain interior (Fig. 5 (c-d)). This recrystallization would be caused by dynamic recrystallization (DRX) during deformation, resulting in improvement of hot ductility at subsolvus temperature. However, focusing on γ′-nodules, only a few recrystallized grains are observed. In addition, as shown in Fig. 6, fractures are often observed in γ′-nodule area (Fig. 6 (a)) and reaction front of γ′-nodule (Fig. 6 (b)) for the 5 K/h-cooled specimen. Hence it is indicated that deformability of γ′-nodule is inferior to grain interior.

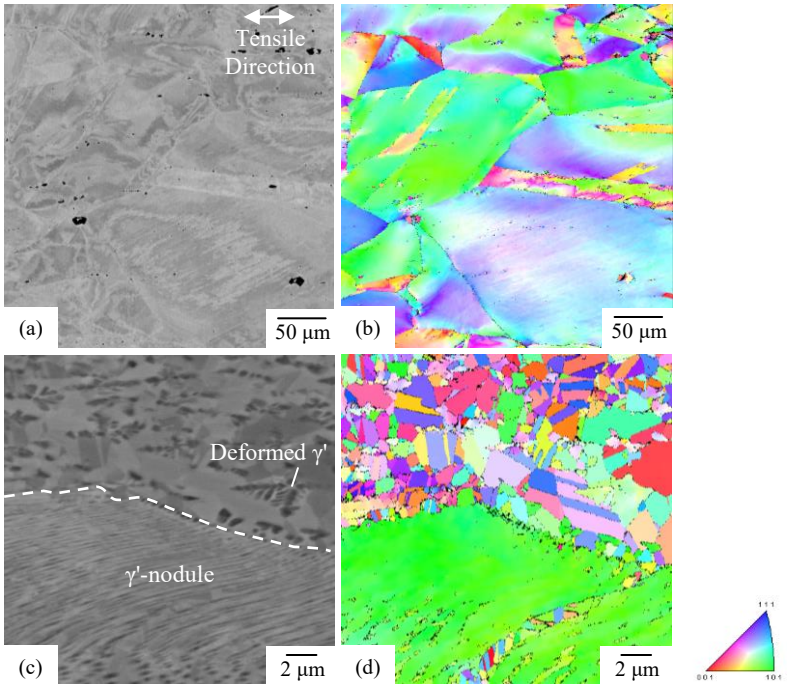

Figure 5: (a), (c) BEIs and (b),(d) corresponding IPF maps for cross-sectional microstructures of the Gleeble test specimens tested at 1173 K:
(a),(b) water-quenched specimen and (c), (d) 10 K/h-cooled specimen.

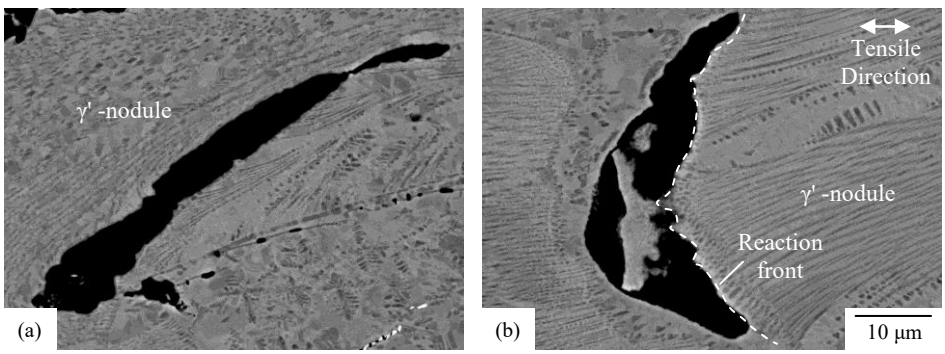

Figure 6: BEIs showing cross-sectional microstructures of the 5 K/h-cooled Gleeble test specimen tested at 1173 K: (a) γ'-nodule area and (b) vicinity of reaction front.

Recrystallization resistance by dispersed secondary particles with a mean diameter of d and area fraction of f_v could be estimated by a value of f_v/d [8]. This value affects the Smith-Zener drag [9], i.e., higher f_v/d value indicates that recrystallization nucleation is suppressed by secondary particles and deformed microstructure is stabilized. Table 3 shows calculated f_v/d values of γ′ precipitates in grain interior for the slow-cooled samples. f_v/d value in grain interior decreases with slowing down the cooling rate in initial cooling process, indicating that slower cooling rate makes better hot ductility since the interparticle spacing is enough to promote DRX. However, the results in Gleeble test showed that reduction of area below γ′-solvus temperature maximized at intermediate cooling rate (20 K/h). It is unable to explain this result without considering the

presence of γ′-nodule. For instance, f_v/d value in γ′-nodule could be estimated to about 1.5 μm^{-1} for the 10 K/h-cooled sample. This value is higher than the value for grain interior by 1 order of magnitude, indicating that DRX is suppressed in γ′-nodule. Thus, as shown in Fig. 7 schematically, the reason why optimal cooling rate exists could be explained by the balance between hot ductility in grain interior and the one in γ′-nodule. The 5 K/h-cooled sample contained too much the γ'-nodule area so that the DRX was suppressed.

Table 3:Average area fraction of γ′-nodule for slow-cooled samples.

Cooling rate	100 K/h	50 K/h	20 K/h	10 K/h	5 K/h
Area fraction of γ′ particles in grain interior, f_v	0.31	0.29	0.26	0.28	0.26
Average diameter of γ′ particle (side length of cubes), d /μm	0.45	0.71	1.11	1.58	2.30
f_v/d /μm^{-1}	0.70	0.41	0.23	0.18	0.11

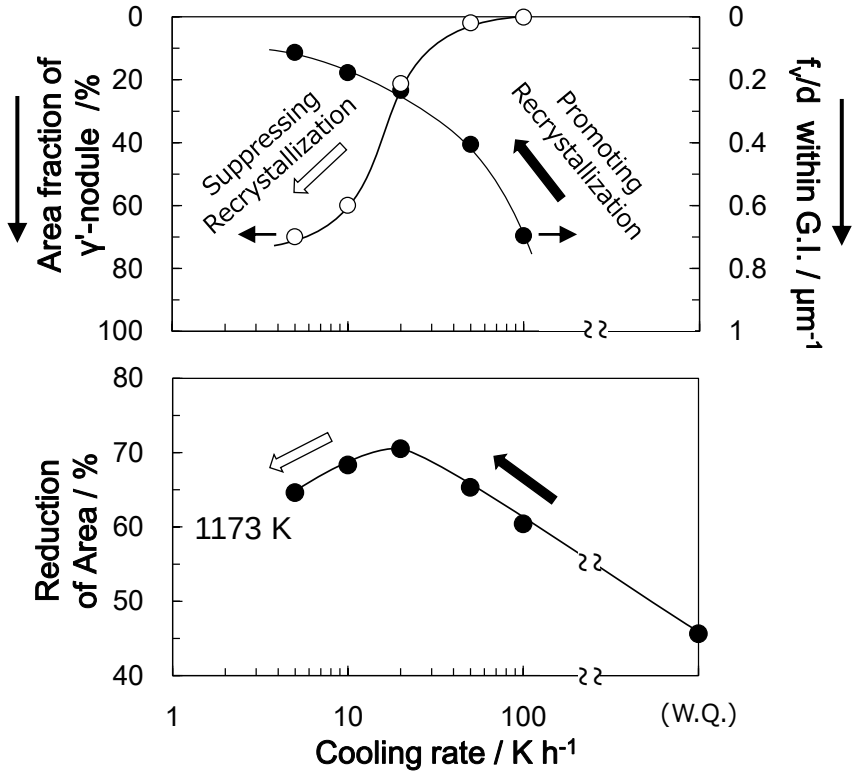

Figure 7: Relationship between microstructural factor and hot ductility at 1173 K as a function of cooling rate in the initial heat-treatment process.

CONCLUSIONS

The relationship between the hot workability and γ′ morphology under the γ′-solvus temperature in Alloy U520 were investigated with a focus on the presence of γ′-nodule. The conclusions obtained are below:

(1) Intragranular γ′ particles and γ′-nodules along grain boundaries are observed after the cooling process from above the γ′-solvus. γ′ precipitates in γ′-nodules show fiber-like or dendritic morphology.
(2) Both the size of intragranular γ′ particle and the area fraction of γ′-nodule increase with decreasing the cooling rate. The area fraction of nodules reaches about 70 % for 5 K/h-cooled sample.
(3) In Gleeble tension test, the slow-cooled samples basically exhibit higher ductility than water-quenched samples below the γ′-solvus temperature. However, the ductility is maximized in the sample cooled at 20 K/h, and excessive decrease of cooling rate results in a drop in ductility.
(4) Dynamic recrystallization is occurred in grain interior but suppressed at γ′-nodule area, indicating that the presence of γ′-nodule had a negative influence on hot workability at subsolvus temperature.

REFERENCES

[1] Zhongnan Bi *et al*, "Solutions for the "difficult-to-deform" wrought superalloys," *MATEC Web of Conferences*, Vol. 14, 07002 (2014).
[2] Danflou, H. L. et al, "Mechanisms of formation of serrated grain boundaries in nickel base superalloys," Superalloys 1996, TMS (1996), pp. 119-127.
[3] Uehara, N. *et al*, "Effect of Heat Treatment on the High Temperature Properties of Udimet 520," *Electric furnace steel*, Vol. 49, No. 4 (1978), pp. 235-241.
[4] Mitchell, R.J. *et al*, "On the formation of serrated grain boundaries and fan type structures in an advanced polycrystalline nickel-base superalloy," *Journal of Materials Processing Technology*, Vol. 209 (2009), pp.1011-1017.
[5] X.D. Lu *et al*, "Effect of slow cooling treatment on microstructure of difficult deformation GH4742 superalloy," *Journal of Alloys and Compounds*, Vol. 477 (2019), pp.100-103.
[6] Susukida, H. *et al*, "Effects of Long-Term Heating on the Strength and Microstructures of Some Gas Turbine Superalloys," *Mitsubishi Juko Giho*, Vol. 9, No. 1 (1972), pp. 102-111.
[7] Schneider, C. A. *et al*, "NIH Image to ImageJ: 25 years of image analysis," *Nature methods*, Vol. 9, No. 7 (2012), pp. 671-675.
[8] John Humphreys *et al*, Recrystallization and Related Annealing Phenomena (Third Edition) , Elsevier (2017), pp. 321-359.
[9] E. Nes *et al*, "ON THE ZENER DRAG," *Acta metallurgica.*, Vol. 33, No. 1 (1985), pp. 11-22.